

Article

Implementation of a Small Type DC Microgrid Based on Fuzzy Control and Dynamic Programming

Chin-Hsing Cheng

Department of Electrical Engineering, Feng Chia University, Taichung 40724, Taiwan; chcheng@fcu.edu.tw; Tel.: +886-4-2451-7250 (ext. 3827)

Academic Editor: Chunhua Liu

Received: 24 July 2016; Accepted: 20 September 2016; Published: 27 September 2016

Abstract: A DC microgrid (DC-MG) is a novel power system that uses DC distribution in order to provide high quality power. The study system is made by a photovoltaic array (PV), a wind generator (WG), a fuel cell (FC), and an energy storage system (ESS) to establish a small type DC microgrid, with the bus being established by DC/DC converters with fuzzy controllers. An overall power dispatch was designed for the proposed system to distribute the power flows among the different energy sources and the storage unit in the system in order to satisfy the load requirements throughout an entire 24-h period. The structure of a power supervisor based on an optimal power dispatch algorithm is here proposed. Optimization was performed using dynamic programming (DP). In this paper, a system configuration of a DC microgrid is analyzed in different scenarios to show the efficacy of the control for all devices for the variable weather conditions with different DC loads. Thus, the voltage level and the power flow of the system are shown for different load conditions.

Keywords: DC microgrid (DC-MG); fuzzy control; dynamic dispatch; energy management; energy storage

1. Introduction

Global environmental concerns and the ever-increasing need for energy, coupled with steady progress in renewable energy technologies, are opening up new opportunities for the utilization of renewable energy resources. Developments of wind and photovoltaic array (PV) energy technologies have increased their use in hybrid wind/PV configurations. Further, integrating of PV and wind energy sources with fuel cells leads to a non-polluting reliable energy source [1].

This paper investigates power flow management for a DC microgrid (DC-MG) with an energy storage system focused on optimal scheduling. The method for performing power management optimization is chosen according to the nature of the problem (components, constraints, and performance index). The main purpose of this work is to find the power flow dispatch that controls for all units through specific converters, especially in case of variable weather conditions with different loads over the studied period. A fuzzy control system tuned by a dynamic programming approach is used to manage the microgrid system.

For ease of implementation, fuzzy controllers with microprocessors have been successfully applied to power converters [2–4] and inverters [5–8]. The design of a fuzzy controller is mainly related to knowledge acquisition, tuning, and the improvement of the optimality and stability of the control system. Tuning the scaling factors, the membership function, and the set of control rules have been proposed recently for tuning the fuzzy controller [9]. The membership function parameters of input variables and output variables in a fuzzy control system are commonly used to conduct proper transformations between the real input data and the universe of the discourses of the fuzzy variables in the system. Sometimes, membership function parameters can be used to fine-tune the performance of the designed system in a similar way to tune a proportional-integral-derivative (PID) controller for a

better dynamic response [10–12]. Thus, fuzzy controllers are used for voltage regulation of the system for all the converters used in the microgrid. A dynamic programming (DP) approach to a problem discretizes the problem's state space and uses a backwards recursion to obtain the optimal value in every state. The state variable describing the problem at a particular stage is defined that it completely describes the process. Given the state of the process at the beginning of a stage, we made a decision that transforms the process to the final state at the end of the stage. The objective was to maximize (or minimize) the expected objective over all stages. DP is a graph-based technique corresponding to the shorter path algorithms. The performance index and the constraints can hold all the natures, and no specific mathematical solver is needed are the advantages of the method. Its high memory needs when the studied period is long and discretized within a small time frame is the weakness of this technique. However, it is not problematic if the computation parameters are well chosen, and the computation time can be reduced by appropriate modifications [13,14].

2. Microgrid Architecture

The studied DC-MG consists of a cluster of generators, a storage system, a load, and power electronic interfaces all connected to the DC grid as shown in Figure 1. The regarded distributed generators (DGs) are a 1.2-W wind generator (WG), a 1.8-W PV, and a 1.0-W fuel cell (FC). A stationary lithium iron phosphate battery (3.2 V, 1100 mAh) composes the energy storage system (ESS) and is used for storing and supplying electrical power. The specifications of these devices are shown in Table 1.

The voltage of the DC bus is set to 10 V in this study. A BUCK converter is used for the PV to decrease the voltage level. A SEPIC converter is used for the WG through a rectifier to regulate the DC voltage. A BOOST converter is used for the FC to increase the voltage level. A bidirectional DC/DC converter is used for the ESS to charge and discharge the energy from the DC bus to balance the power flow and stabilize the voltage level. The deviation of power of each DG is obtained by the measured current (i) and the deviation of voltage (ΔV). Each of the four fuzzy logic controllers (FLCs) has two inputs, the deviation of load power (ΔP_{load}), and the deviation of converter power (ΔP_{DG}). The output of each FLC is the control signal of duty cycle ($\Delta duty$). The experiment was executed on a personal computer (PC). The A/D converter was used to convert the analog output voltage of the DC/DC converter into digital data, and a D/A converter was used to convert the digital results calculated by the PC into an analog control signal. The analog control signal was fed into ICs TL494 for a pulse width modulation (PWM) to generate the appropriate duty cycle.

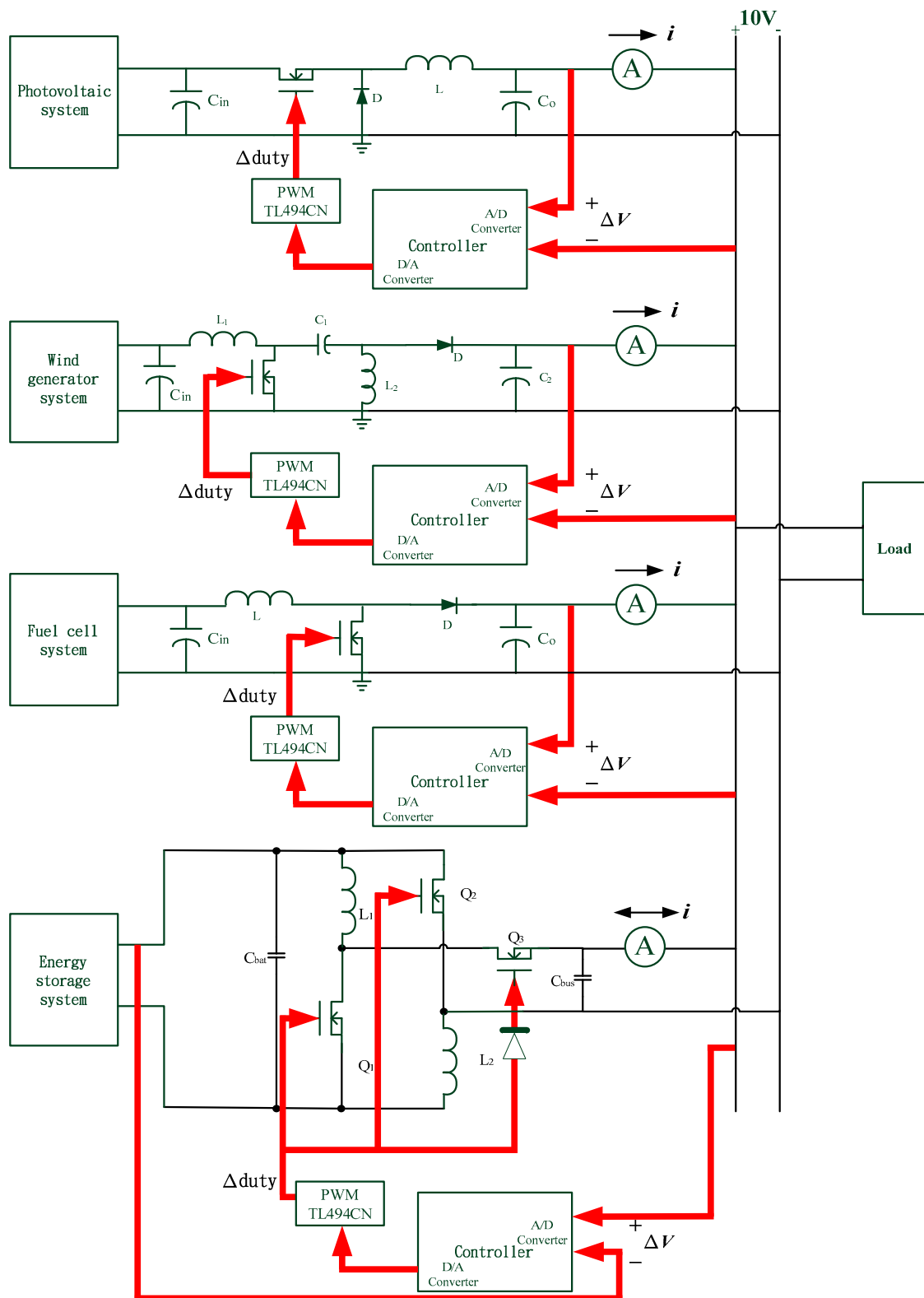
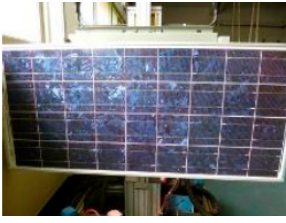





Figure 1. Microgrid architecture.

Table 1. Specifications of the devices.

<p>PV</p> 	<p>BP365, 12-V, 65-W PV Module (When exposed to sunlight, it will generate 12 V of DC power into a battery, up to a maximum of 65 W according to the strength of solar radiation.)</p>
<p>WG</p> 	<p>Rutland WG913 Windcharger (1 × Main Generator Assembly, 6 × Aerofoil Blades). The 12 V of DC power generated relates directly to the wind speed at the turbine.</p>
<p>FC/cell</p> 	<p>Size (L × W × H: 65 × 85 × 38 mm), maximum power of 0.25 W, maximum current of 1 A, maximum voltage of 0.9 V.</p>
<p>ESS</p> 	<p>IRF18650P, Lithium iron phosphate battery (3.2 V, 1100 mAh).</p>

3. Fuzzy Logic Controller and Dynamic Programming

3.1. Fuzzy Logic Controller (FLC)

There are four steps for the design of FLC:

Step 1: Defining the Model's Functional and Operational Characteristics

Defining exactly where the fuzzy subsystem fits into the total system architecture, which helps the designer to estimate the numbers and ranges of inputs and outputs that will be required is the essential step.

Step 2: Designing the Fuzzifier

Mapping from an observed input space to fuzzy sets in certain input universes of discourse is the fuzzification interface performed by the fuzzifier. This strategy interprets a crisp value x as a fuzzy set A with membership function $\mu_{A(x)}$ belonging to $[0, 1]$. Each variable in the fuzzy model is divided into

a set of fuzzy regions, which are given unique names, with labels such as “positive big”, “negative small”, “cool”, “slow”, etc. These labels are related to the physical states of the fuzzy variable.

Step 3: Designing the Inference Engine

This step involves writing the rules with syntax, e.g., IF <fuzzy proposition> THEN <fuzzy proposition>. The fuzzy proposition might be originally written in English, e.g., IF the change of load power is decreasing very much and the change of DG power is also decreasing very much, THEN the change of duty of the system shall be decreased greatly. Thus, the statement of the rule will be IF ΔP_{load} is NB and ΔP_{DG} is NB THEN $\Delta duty$ is NB. There are five methods to generate fuzzy control rules. These methods are not mutually exclusive, and it seems likely that a combination of them may be necessary to construct an effective method for the derivation of fuzzy control rules. These methods are (1) expert experience and knowledge; (2) modeling the operator’s control actions; (3) modeling the process; (4) self-organization; and (5) learning from numerical examples.

Step 4: Selecting a Defuzzification Method

The final step of creating the FLC is the selection of the defuzzification interface. There are several ways to convert an output fuzzy set into a crisp variable, but the most commonly used strategies include max criterion, mean of maximum method (MOM), and center of area method (COA). The COA method is used in this paper to generate the center of gravity of the possibility distribution of a control action. The method considers both membership function value and its shape. In the case of two-inputs (x_1, x_2) and one-output (y),

$$y_{crisp} = \frac{\sum_{i=1}^N \mu_{(A_i \cap B_i)}(x_1, x_2) \cdot \bar{y}_i}{\sum_{i=1}^N \mu_{(A_i \cap B_i)}(x_1, x_2)},$$

where N is the total number of fuzzy rules, \bar{y}_i denotes the center value of the output set in their domain, which is fired at the i th fuzzy rule, and μ_{A_i} (μ_{B_i}) is the grade of membership at which x_1 and x_2 belong to the sets A_i (B_i).

All membership functions (MFs) of each of the FLC inputs and outputs are defined on the common normalized domain $[0, 1]$, as shown in Figures 2–4. The acronyms NB, NS, ZE, PS, and PB stand for negative big, negative small, zero, positive small, and positive big, respectively. Here, triangular MFs are chosen for all fuzzy sets. The fuzzy rules for ΔP_{load} and ΔP_{DG} are shown in Table 2.

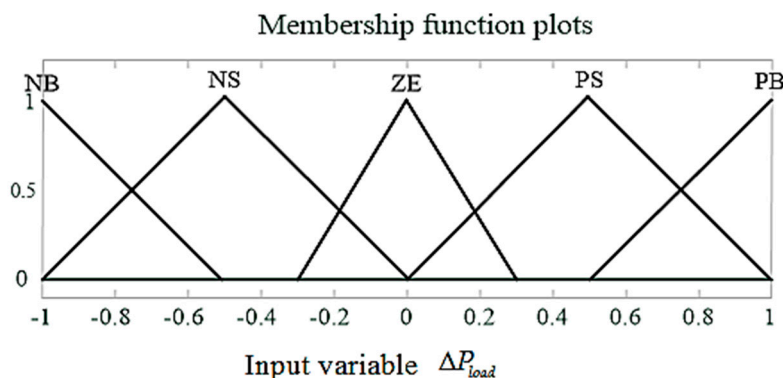


Figure 2. Normalized membership function of the ΔP_{load} .

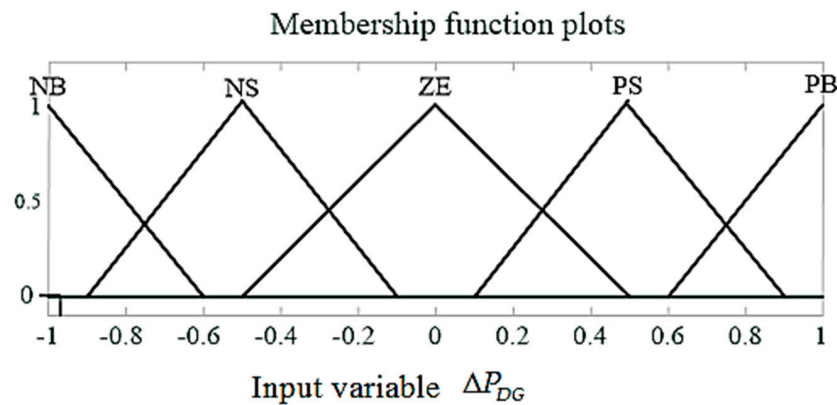


Figure 3. Normalized membership function of the ΔP_{DG} .

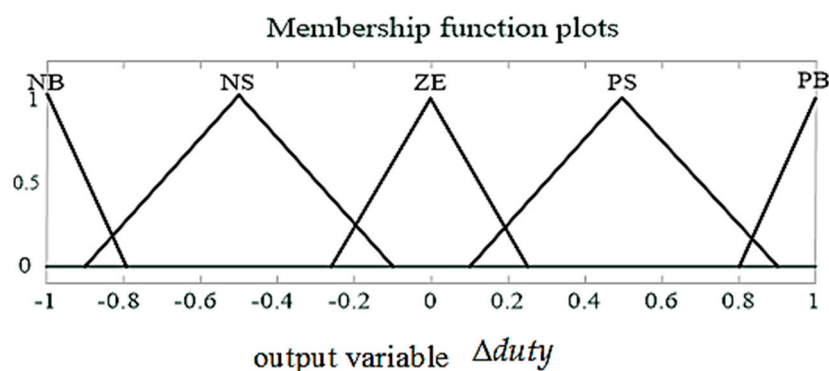


Figure 4. Normalized membership function of the control signal.

Table 2. Fuzzy rules for ΔP_{load} and ΔP_{DG} .

$\Delta P_{DG} \backslash \Delta P_{load}$	NB	NS	ZE	PS	PB
NB	NB	NB	NS	PS	PS
NS	NB	NB	NS	PS	PS
ZE	NB	NS	ZE	PS	PB
PS	NB	NS	PS	PB	PB
PB	NS	NS	PS	PB	PB

3.2. Dynamic Programming (DP)

DP was used to solve the optimization problem. The problem was formulated as a system evolution divided into a multi-stage decision process. To illustrate the type of functional equation that arises from an application of the principle of optimality, begin with the simplest case of a deterministic process where the system is described at any time by an M -dimensional vector $p = (p_1, p_2, \dots, p_M)$, constrained to lie within some region D . Let $F = \{F_k\}$, where k runs over a set which may be finite, enumerable, or continuous, be a set of transformations with the property that $p \in D$ implies that $F_k(p) \in D$ for all k .

Assume that an N -stage process are considered to be carried out to maximize some scalar function, $S(p)$ of the final state. This function is called the N -stage return. A policy consists of a selection of N transformations, where $p = (F_1, F_2, \dots, F_N)$, yielding successively the states

$$\begin{aligned}
 p_1 &= F_1(p), \\
 p_2 &= F_2(p_1), \\
 &\dots, \\
 p_N &= F_N(p_{N-1}).
 \end{aligned}
 \tag{1}$$

If D is a finite region, if each $F_k(p)$ is continuous in p , and if $S\{p\}$ is a continuous function of p for $p \in D$, it is clear that an optimal power exists. The maximum value of $S(p_N)$, determined by an optimal power, will be a function only of the initial vector p and the number of stages N . Let us then define

$$P_{f_N}(p) = \underset{p}{\text{MAX}} S(p_N), \tag{2}$$

This is the N -stage return obtained using an optimal power starting from the initial state p .

To derive a functional equation for $P_{f_N}(p)$, we employ the principle cited above. Assuming that we choose some transformation F_k as a result of our first decision, thereby obtaining a new state $F_k(p)$, the maximum return from the following $(N-1)$ stages is, by definition, $P_{f_{N-1}}(F_k(p))$. It follows that k must now be chosen so as to maximize this result, the basic functional equation being

$$P_{f_N}(p) = \underset{k}{\text{MAX}} P_{f_{N-1}}(F_k(p)), \quad N = 2, 3, \dots \tag{3}$$

It is clear that a knowledge of any particular optimal power will yield $P_{f_N}(p)$, which is unique. Conversely, given the sequence $\{P_{f_N}(p)\}$, all optimal powers may be determined [15].

The constraints of the generated power of DGs are as follows:

$$P_{PV} \leq P_{PV_MAX} = 1.8W, \tag{4}$$

$$P_{WG} \leq P_{WG_MAX} = 1.2 \text{ W, and} \tag{5}$$

$$P_{FC} \leq P_{FC_MAX} = 1.0W, \tag{6}$$

where P_{PV} is the generated power by PV, P_{WG} is the generated power by WG, and P_{FC} is the generated power by FC.

There are i ($i = 0-4$) stages between time $(t-1)$ and time t . The stages relation table is shown in Table 3. The DP models are described by the following equations.

$$P_{f_3}(s) = P_{FC}(x_i), \tag{7}$$

$$P_{f_2}(s) = \underset{x_i=0,1,\dots,4}{\text{MAX}} \{P_{WG}(x_i) + P_{f_3}(s-x_i)\}, \text{ and} \tag{8}$$

$$P_{f_1}(s) = \underset{x_i=0,1,\dots,4}{\text{MAX}} \{P_{PV}(x_i) + P_{f_2}(s-x_i)\}, \tag{9}$$

where $P_{f_3}(s)$ is only determined by FC. $P_{f_2}(s)$ is determined by WG and $P_{f_3}(s)$. $P_{f_1}(s)$ is determined by PV and $P_{f_2}(s)$.

The detailed computing procedures are as follows:

$$P_{f_3}(0) = P_{FC}(x_0), \tag{10}$$

$$P_{f_3}(1) = P_{FC}(x_1), \tag{11}$$

$$P_{f_3}(2) = P_{FC}(x_2), \tag{12}$$

$$P_{f_3}(3) = P_{FC}(x_3), \text{ and} \tag{13}$$

$$P_{f_3}(4) = P_{FC}(x_4). \tag{14}$$

The following equations can be obtained by substituting Equation (8) with Equations (10)–(14).

$$P_{f_2}(0) = P_{WG}(x_0) + P_{f_3}(0), \quad (15)$$

$$P_{f_2}(1) = \text{MAX} \{P_{WG}(x_0) + P_{f_3}(1), P_{WG}(x_1) + P_{f_3}(0)\}, \quad (16)$$

$$P_{f_2}(2) = \text{MAX} \{P_{WG}(x_0) + P_{f_3}(2), P_{WG}(x_1) + P_{f_3}(1), P_{WG}(x_2) + P_{f_3}(0)\}, \quad (17)$$

$$P_{f_2}(3) = \text{MAX} \{P_{WG}(x_0) + P_{f_3}(3), P_{WG}(x_1) + P_{f_3}(2), P_{WG}(x_2) + P_{f_3}(1), P_{WG}(x_3) + P_{f_3}(0)\}, \text{ and} \quad (18)$$

$$P_{f_2}(4) = \text{MAX} \{P_{WG}(x_0) + P_{f_3}(4), P_{WG}(x_1) + P_{f_3}(3), P_{WG}(x_2) + P_{f_3}(2), P_{WG}(x_3) + P_{f_3}(1), P_{WG}(x_4) + P_{f_3}(0)\}. \quad (19)$$

The following equations can be obtained by substituting Equation (9) with Equations (15)–(19).

$$P_{f_1}(0) = P_{PV}(x_0) + P_{f_2}(0), \quad (20)$$

$$P_{f_1}(1) = \text{MAX} \{P_{PV}(x_0) + P_{f_2}(1), P_{PV}(x_1) + P_{f_2}(0)\}, \quad (21)$$

$$P_{f_1}(2) = \text{MAX} \{P_{PV}(x_0) + P_{f_2}(2), P_{PV}(x_1) + P_{f_2}(1), P_{PV}(x_2) + P_{f_2}(0)\}, \quad (22)$$

$$P_{f_1}(3) = \text{MAX} \{P_{PV}(x_0) + P_{f_2}(3), P_{PV}(x_1) + P_{f_2}(2), P_{PV}(x_2) + P_{f_2}(1), P_{PV}(x_3) + P_{f_2}(0)\}, \text{ and} \quad (23)$$

$$P_{f_1}(4) = \text{MAX} \{P_{PV}(x_0) + P_{f_2}(4), P_{PV}(x_1) + P_{f_2}(3), P_{PV}(x_2) + P_{f_2}(2), P_{PV}(x_3) + P_{f_2}(1), P_{PV}(x_4) + P_{f_2}(0)\}. \quad (24)$$

The maximum load power can be obtained by the maximum value of $P_{f_1}(X)$ ($X=0-4$). The power distributions of PV, WG, and FC can be obtained by backward substitutions from these equations.

Table 3. The stages relation table.

i	$P_{PV}(x_i)$	$P_{WG}(x_i)$	$P_{FC}(x_i)$
0	$P_{PV}(x_0)$	$P_{WG}(x_0)$	$P_{FC}(x_0)$
1	$P_{PV}(x_1)$	$P_{WG}(x_1)$	$P_{FC}(x_1)$
2	$P_{PV}(x_2)$	$P_{WG}(x_2)$	$P_{FC}(x_2)$
3	$P_{PV}(x_3)$	$P_{WG}(x_3)$	$P_{FC}(x_3)$
4	$P_{PV}(x_4)$	$P_{WG}(x_4)$	$P_{FC}(x_4)$

4. Experimental Results

For the satisfactory operation of the DC microgrid during the variations of photovoltaic generation, wind generation, fuel cell generation, and load conditions, there are a number of different operation modes that need to be considered in order to ensure a secure and reliable power supply. The following paragraph describes the three experimental scenarios.

Case A: On a cloudy day, the PV is out of service. At 0:00, the system energy is supplied by the WG and the FC, each supplying 350 mW, with the load demand of only 168 mW. Thus, the extra energy is stored in the ESS. At 6:00, the load demand increases, and continues to be supplied by the WG and the FC. At 11:00, the load demand decreases, and the ESS is not full, so some of energy is stored in the ESS. At 14:00, as the load demand increases, the WG must increase its output to balance the power flow. At 16:00, the ESS is full, causing the WG to decrease its output. At 18:00, the load demand increases, causing the output of the WG to also increase. At 21:00, the load demand further decreases, causing the output of the WG to decrease as well. The voltage level and the power flow in the MG are shown in Figures 5 and 6.

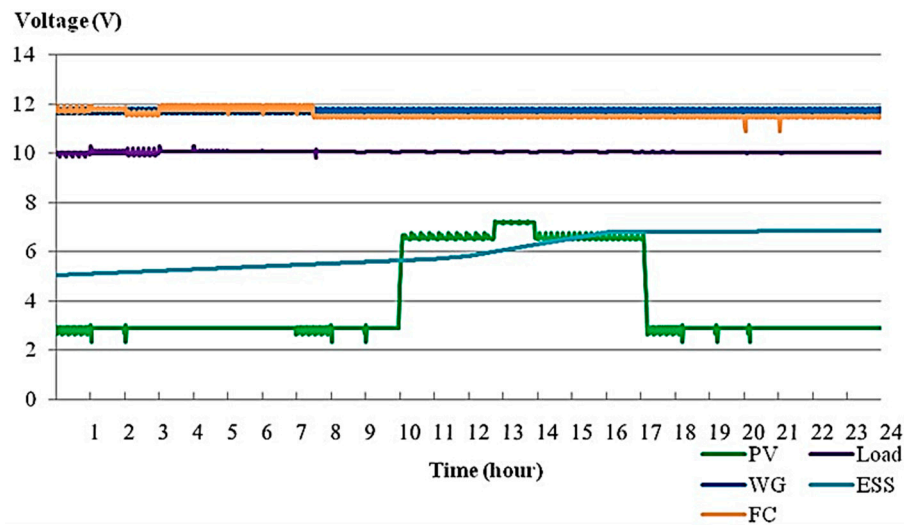


Figure 5. The voltage levels in the microgrid (MG) for case A.

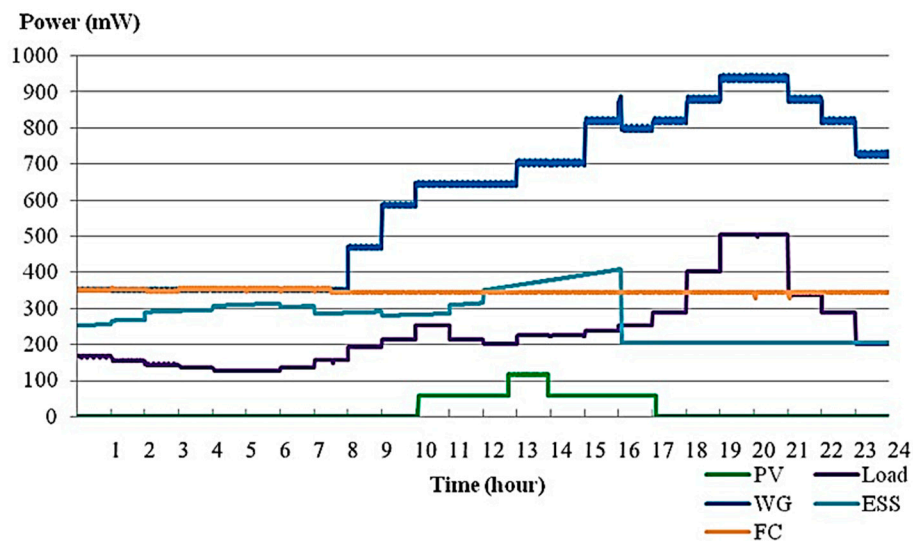


Figure 6. The power flows in the MG for case A.

Case B: At 0:00, there is no wind, the load demand is supplied by the FC, and the extra energy is stored in the ESS. At 8:00, the load demand increases, causing the PV and the WG to supply the load demand simultaneously. At 12:00, the load demand decreases and the ESS is not full, and some of energy is stored in the ESS. At 14:00, the load demand increases, and the PV and the WG are out of service, causing the output of the FC increases. At 19:00, the load demand increases, the FC cannot satisfy the load demand, causing the ESS to provide the output power. At 20:00, the load demand decreases, causing the FC to supply the load demand and the ESS to stop providing the output power. The voltage level and the power flow in the MG are shown in Figures 7 and 8.

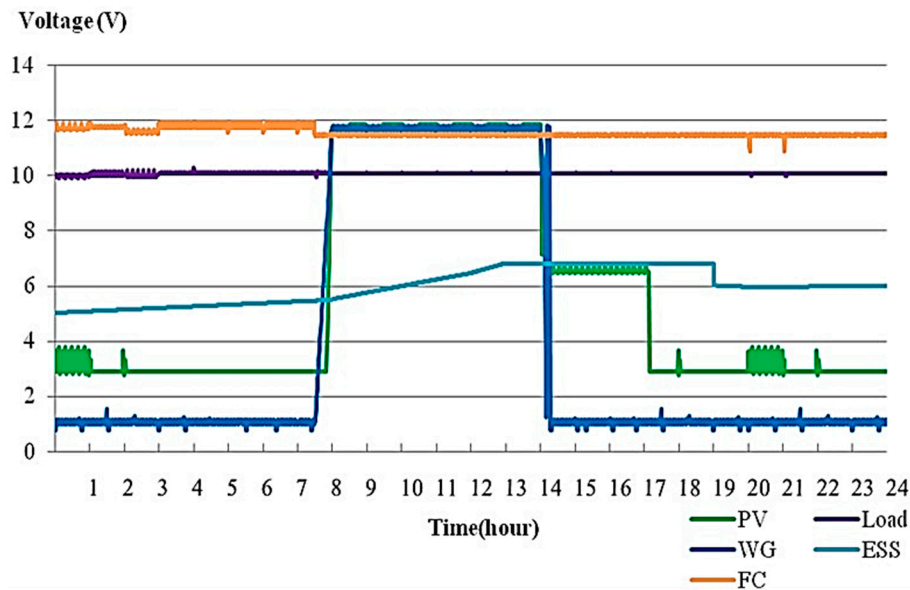


Figure 7. The voltage levels in the MG for case B.

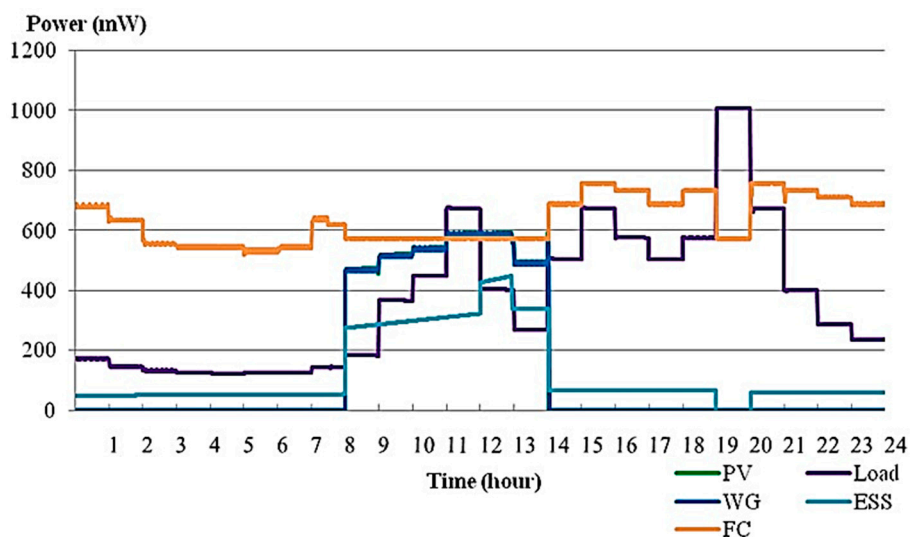


Figure 8. The power flows in the MG for case B.

Case C: At 0:00, due to the lower load demand, the load demand is sufficiently supplied by the FC. At 8:00, the PV becomes the main source of energy due to the sun light. At time 9:00, the WG also supplies the energy. Since the PV is the main source, the WG is the slave source. Extra energy is used to charge the ESS. At 12:00, the load demand decreases, causing the charge rate of the ESS to increase. At 14:00, the load demand increases, causing the used power to charge, the ESS is switched to the load to balance the power. At 15:00, the ESS is full. At 18:00, the PV cannot supply the power due to a lack of sunlight, and the WG becomes the main power. At 20:00, the WG cannot supply the power due to a lack of wind. The FC becomes the main power. The shortage of power, causes the stored power in the ESS to switch to discharge power to supply load demand. The voltage level and the power flow in the MG are shown in Figures 9 and 10.

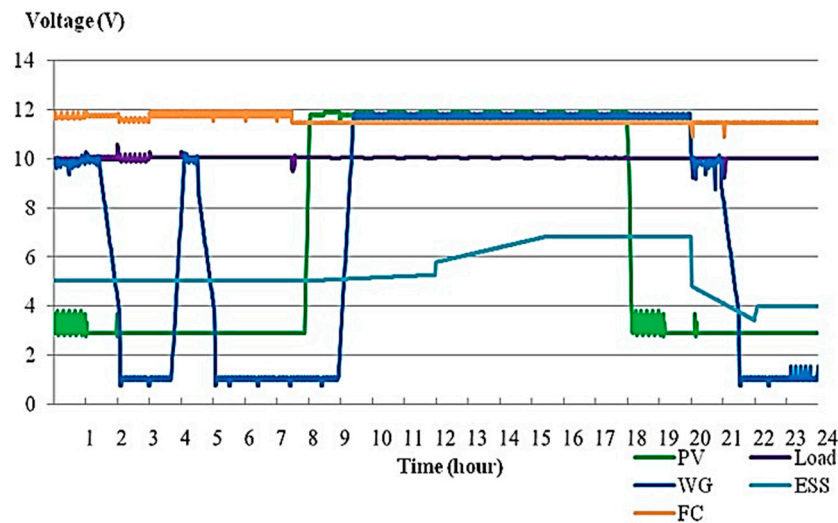


Figure 9. The voltage levels in the MG for case C.

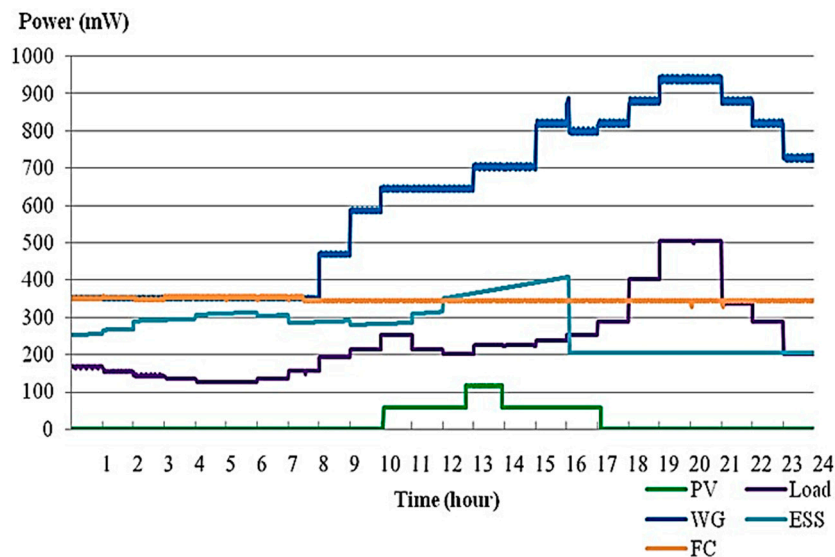


Figure 10. The power flows in the MG for case C.

5. Conclusions

In this paper, we propose the concept of a small type DC microgrid and show a system configuration and control methods for power converters and generators. A DC-MG-based power generation system with a PV, WT, GE, and ESS generation that is connected to the grid is proposed. During islanded operation, the power and voltage of a microgrid may change rapidly due to a power imbalance between supply and demand. Fuzzy controllers and a dynamic programming method are suggested in order to increase the injected power and balance the power flow and the voltage level of the distributed generators. The energy storage system is also considered to overcome the power flow issue and stabilize the voltage level. The experimental results show that the proposed control method provides good operation performance for different load conditions.

Acknowledgments: This work was supported by the Ministry of Science and Technology of Taiwan, Republic of China, under Grant number MOST 103-2221-E-035-039.

Conflicts of Interest: The author declares no conflict of interest.

References

1. El-Shatter, T.F.; Eskander, M.N.; El-Hagry, M.T. Energy flow and management of a hybrid wind/PV/fuel cell generation system. *Energy Convers. Manag.* **2006**, *47*, 1264–1280. [[CrossRef](#)]
2. Gupta, T.; Boudreaux, R.R.; Nelms, R.M.; Hung, J.Y. Implementation of a fuzzy controller for DC-DC converters using an inexpensive 8-b microcontroller. *IEEE Trans. Ind. Electron.* **1997**, *44*, 661–669. [[CrossRef](#)]
3. Balestrino, A.; Landi, A.; Sani, L. Cuk converter global control via fuzzy logic and scaling factors. *IEEE Trans. Ind. Appl.* **2002**, *38*, 406–413. [[CrossRef](#)]
4. Cheng, C.H.; Cheng, P.J.; Wu, M.T. Fuzzy logic design of self-tuning switching power supply. *Expert Syst. Appl.* **2010**, *37*, 2929–2936. [[CrossRef](#)]
5. Osterholz, D.I.H. Simple fuzzy control of a PWM inverter for a UPS system. In Proceedings of the 17th International Telecommunications Energy Conference, Den Haag, The Netherlands, 29 October–1 November 1995; pp. 565–570.
6. Lin, B.R. Analysis of neural and fuzzy power electronic control. *IEE Proc. Sci. Meas. Technol.* **1997**, *144*, 25–33. [[CrossRef](#)]
7. Tzou, Y.Y.; Ho, L.H.; Ou, R.S. Fuzzy control of a closed-loop regulated PWM inverter under large load variations. In Proceedings of the IEEE IECON, Lahaina, HI, USA, 15–19 November 1993; pp. 267–272.
8. Cheng, C.H. Design of output filter for inverters using fuzzy logic. *Expert Syst. Appl.* **2011**, *38*, 8639–8647. [[CrossRef](#)]
9. Maeda, M.; Murakami, S. A self-tuning fuzzy controller. *Fuzzy Sets Syst.* **1992**, *51*, 29–40. [[CrossRef](#)]
10. Chen, Y.K.; Yang, C.H.; Wu, Y.C. Robust fuzzy controlled photovoltaic power inverter with Taguchi method. *IEEE Trans. Aerosp. Electron. Syst.* **2002**, *38*, 940–954. [[CrossRef](#)]
11. Kim, J.Y.; Kim, H.M.; Kim, S.K.; Jeon, J.H.; Choi, H.K. Designing an Energy Storage System Fuzzy PID Controller for Microgrid Islanded Operation. *Energies* **2011**, *4*, 1443–1460. [[CrossRef](#)]
12. Khairy, S.; Hossam, A.G. Electric Vehicle to Power Grid Integration Using Three-Phase Three-Level AC/DC Converter and PI-Fuzzy Controller. *Energies* **2016**, *9*, 532.
13. Riffonneau, Y.; Bacha, S.; Barruel, F.; Ploix, S. Optimal Power Flow Management for Grid Connected PV Systems with Batteries. *IEEE Trans. Sustain. Energy* **2011**, *2*, 309–320. [[CrossRef](#)]
14. Mokrian, P.; Stephen, M. A Stochastic Programming Framework for the Valuation of Electricity Storage. In Proceedings of the 26th USAEE/IAEE North American Conference, Ann Arbor, MI, USA, 24–27 September 2006.
15. Bellman, R. The theory of dynamic programming. *Proc. Natl. Acad. Sci. USA* **1952**, *60*, 503–715. [[CrossRef](#)]



© 2016 by the author; licensee MDPI, Basel, Switzerland. This article is an open access article distributed under the terms and conditions of the Creative Commons Attribution (CC-BY) license (<http://creativecommons.org/licenses/by/4.0/>).